Chapter 3
Geochemical Properties

Abstract Shale reservoirs with organic-rich intervals are often characterized by high quantities of kerogen, bitumen and also moveable hydrocarbons. Despite lots of conducted studies to improve understanding of the shale characteristics, kerogen, as one the main constituents of mudrocks, is not thoroughly understood. Understanding organic matter properties in terms of maturity, content, and type are crucial for the development of unconventional reservoirs. Studies also showed the presence of organic matter has a non-negligible effect on hydraulic fracturing operations. In this chapter, organic matter characterization by conventional methods along with a new analytical method known as Raman spectroscopy are discussed.

3.1 Characterizing Geochemical Properties of Organic Matter

Organic matter, predominantly kerogen, is formed from the burial and preservation of living organisms and is interspersed within the mineral matrix (Hutton et al. 1994), Fig. 3.1. In order to study organic matter properties, bulk sample, Fig. 3.1a, or isolated kerogen, Fig. 3.1b–d, can be used. Rock-Eval pyrolysis, vitrinite reflectance, infrared and Raman spectroscopy, elemental analysis, and X-ray absorption near edge structure are some techniques for evaluating the organic matter. Parameters that are mostly considered are: maturity level, hydrogen and oxygen richness, total organic content, aromaticity of kerogen structure, and potential to produce hydrocarbon which are discussed in the following sections.

The main method to understand the thermal maturity of kerogen is the optical inspection of vitrinite macerals, known as vitrinite reflectance (Diessel et al. 1978). Vitrinite reflectance analysis can be challenging when samples contain dispersed or no primary vitrinite (Hackley et al. 2015; Sauerer et al. 2017), Fig. 3.2. In order to find the maturity for these samples, a mean of bitumen maturity (%Bro) can be used

M. Ostadhassan et al., *Fine Scale Characterization of Shale Reservoirs*,
SpringerBriefs in Petroleum Geoscience & Engineering,
https://doi.org/10.1007/978-3-319-76087-2_3

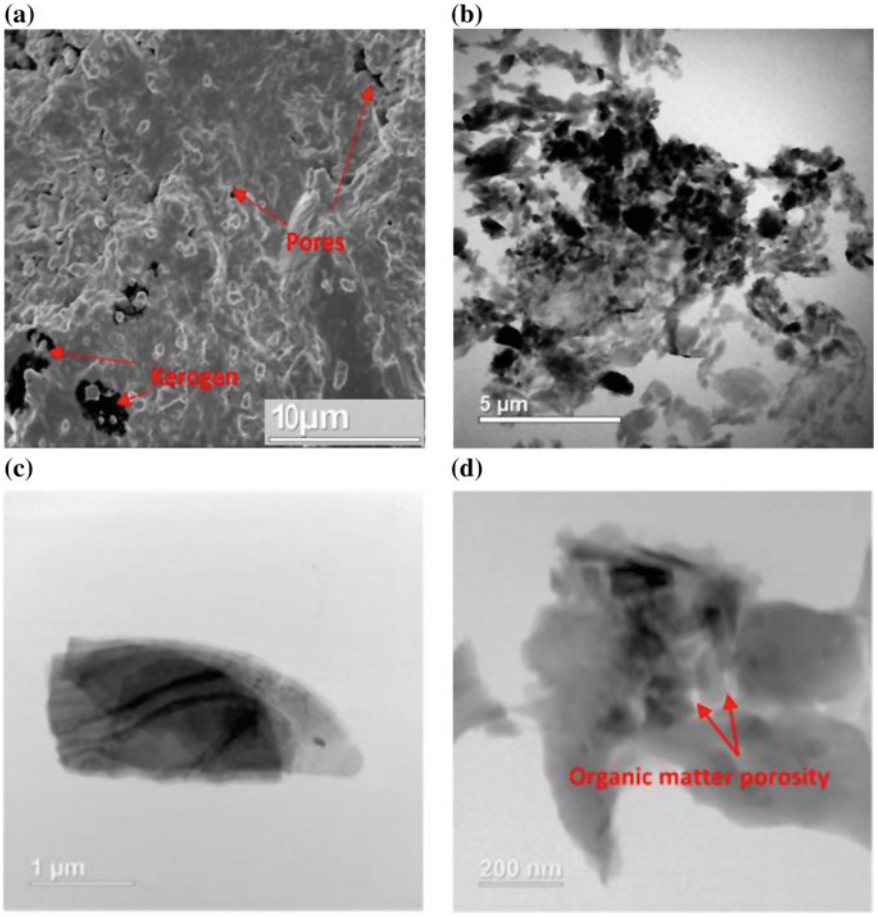

Fig. 3.1 **a** SEM images of Bakken shale sample, **b–d** STEM image of isolated kerogen at different scales

to obtain an equivalent vitrinite maturity (%VRo). This can be done by using linear Equation proposed by Jacob (1989) or converting T_{max} from Rock-Eval (Table 3.1) to %VRo through Eq. 3.2 (Jarvie et al. 2001).

$$\%VRo = \%BRo * 0.618 + 0.4 \tag{3.1}$$

$$\%VRo = 0.0180 * T_{max} - 7.16 \tag{3.2}$$

The common methods for evaluating organic matter properties are LECO, Rock-Eval pyrolysis, and organic petrography by microscopic methods. Rock-Eval (RE) pyrolysis is a universally accepted analysis in which a sample is subjected to a programmed heating (Espitalie et al. 1985; Peters 1986; Behar et al. 2001).

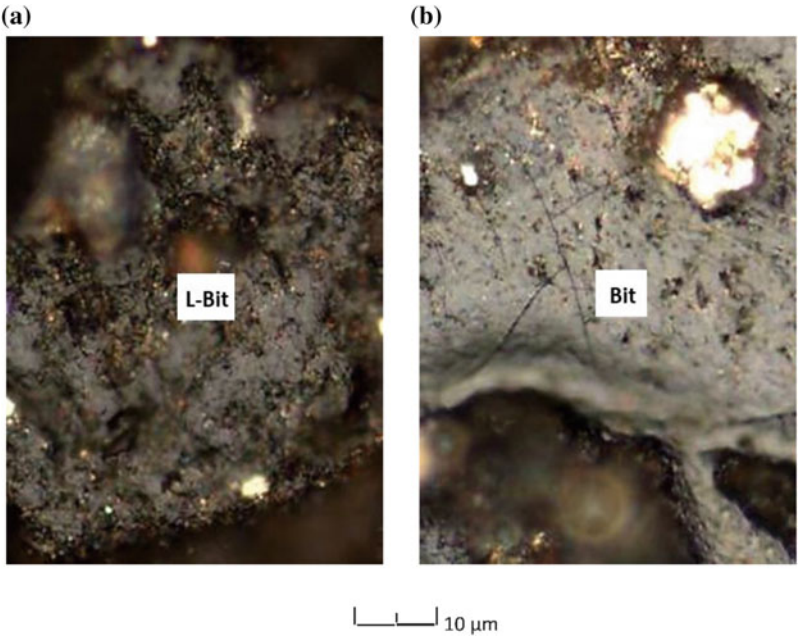

Fig. 3.2 **a**, **b** Two samples with organic matter comprises primary low-reflecting bitumen (L-B) bitumen (Bit), while no reliable grain of primary vitrinite is encountered

Table 3.1 Direct and derived parameters from Rock-Eval

Direct measurements		Derived measurements	
S1	Presents the already generated oil in the rock which will be distilled out of the sample at initial heating of the sample (350 °C)	TOC	Known as total organic carbon and is calculated as the sum of pyrolyzed OC and residual OC
S2	Presents the amount of hydrocarbon generated through thermal cracking of kerogen (550 °C). S2 is hydrocarbon which potentially will be produced	HI	Is the ratio of S_2 to TOC as a measure of the hydrogen richness of the source rock
S3	Is the trapped CO_2 released during pyrolysis (up to 390 °C) which is proportional to the oxygen presents in the kerogen	OI	Is the ratio of S_3 to TOC as a measure of the oxygen richness of the source rock

(continued)

Table 3.1 (continued)

Direct measurements		Derived measurements	
S4	Is the residual carbon content of a sample, with little or no potential to generate hydrocarbons	PI	Known as production index which is the ratio of already generated hydrocarbon (S1) to the total potential of hydrocarbon (S1 + S2). Low ratios indicate either immaturity or extreme post-mature organic matter. High ratios are interpreted as the mature stage or contamination by drilling additives or migrated hydrocarbons
T_{max}	Is the temperature at the top of the S2 peak (maximum release of hydrocarbons during pyrolysis). It is an indicator of thermal maturity	OSI	Known as oil saturation index which is the potential oil flow zones in shale reservoirs. The higher OSI, the higher chance of production. The main reason for using OSI rather than TOC for evaluating the real potential of shale oil reservoir is that OSI considers the fraction of TOC that contains moveable hydrocarbon

The Rock-Eval process results in different parameters in which some are directly measured, and some can be derived from the results (Lafargue et al. 1998; Carvajal-Ortiz and Gentzis 2015), Table 3.1.

Using parameters yield from Rock-Eval, different plots can be generated to graphically show Kerogen type, its potential to produce hydrocarbon, quality and its position in gas/oil window, such as in Fig. 3.3.

The complexity of shale plays in terms of constituent components has demonstrated that new analytical methods should be acquired to better understand hydrocarbon generation processes. One of the new methods for characterizing organic rich shales is Raman spectroscopy. Raman spectroscopy, based on molecular vibration, can provide chemical composition information of samples. Structural changes of organic matter while maturation process can be monitored by Raman spectroscopy and yields valuable information in terms of organic matter properties. In the following section, the ability of Raman spectroscopy on the characterization of organic matter is discussed.

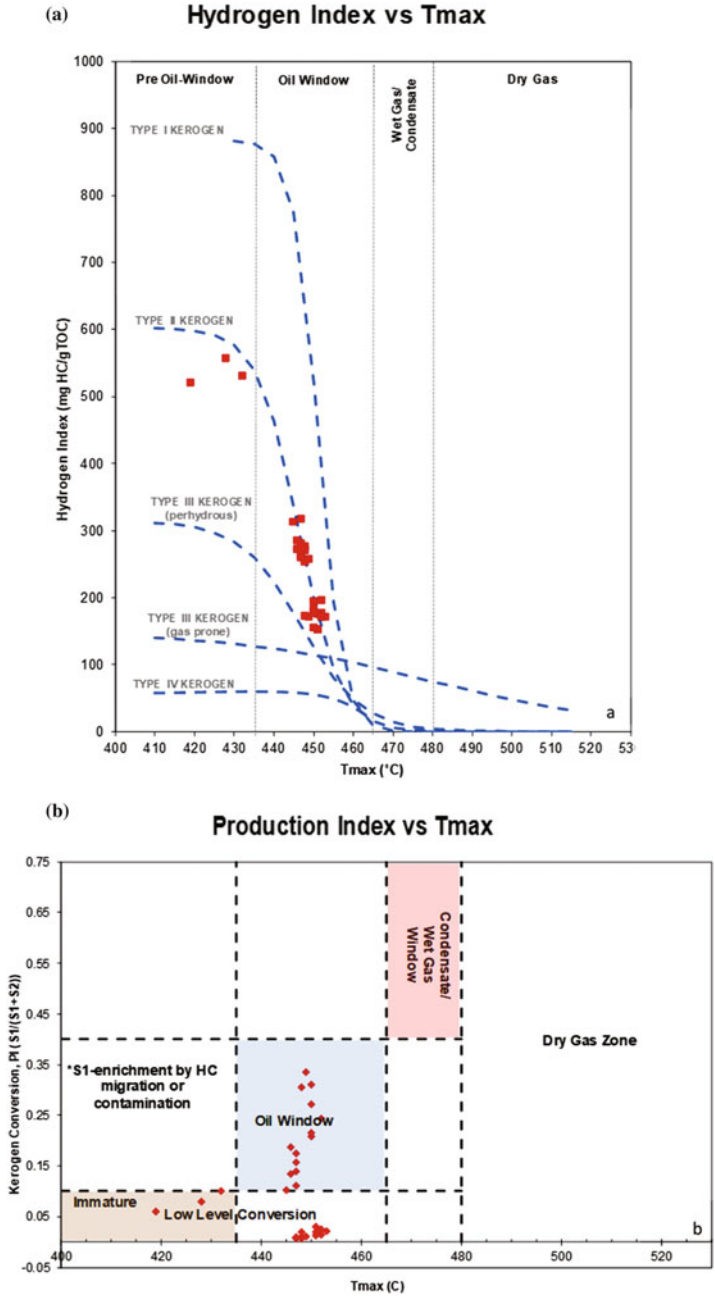

Fig. 3.3 **a** Hydrogen index versus T_{max} for kerogen type, **b** PI versus T_{max} for finding the level of kerogen conversion

3.2 Raman Spectroscopy

In Raman spectroscopy, the sample is irradiated by intense laser beams in the UV-visible region, and the scattered light is usually observed in the direction perpendicular to the incident beam. The scattered light consists of two types: one, called Rayleigh scattering, is strong and has the same frequency as the incident beam (i_f), and the other, called Raman scattering, is very weak (almost 10^{-5} of the incident beam) and has frequencies $i_f \pm m_f$, where m_f is a vibrational frequency of a molecule. Thus, in Raman spectroscopy, we measure the vibrational frequency as a shift from the incident beam frequency (Reich and Thomsen 2004; Amer 2009).

In diatomic molecules, the vibration occurs only along the chemical bond connecting the nuclei. In polyatomic molecules, the situation is complicated because all the nuclei perform their own harmonic oscillations. However, we can show that any of these complicated vibrations of a molecule can be expressed as a superposition of a number of "normal vibrations" that are completely independent of each other (Mitra 1962).

The Raman spectrum of kerogen consists of two main peaks known as G and D bands (Cesare and Maineri 1999; Marshall et al. 2010; Tuschel 2013), Fig. 3.4a. The G band refers to graphite, which appears at approximately 1600 cm^{-1} with a sharp peak. The origin of the G band is due to the inplane E_{2g2} vibrational modes of the carbon atoms in aromatic ring structures (sp^2 carbon) exhibiting D^4_{6h} symmetry (Sauerer et al. 2017). The D band refers to a disorder in the atoms which appears around 1350 cm^{-1} as a narrow peak which is a result from the Raman-active A_{1g} symmetry associated with lattice defects and discontinuities of the sp^2 carbon network (Sauerer et al. 2017; Khatibi et al. 2018). In some literature, two more minor defect bands are also detected around 1510 and 1625 cm^{-1} (Beyssac et al. 2002; Huang et al. 2010). It is worth mentioning that, Raman spectroscopy can also show the presence of other components present in organic rich shale such as Calcium carbonate, Titanium dioxide, Pyrite and Dolomite as discussed by Tuschel (2013), Fig. 3.4b, c, which is out of scope of this book.

3.3 Raman Spectroscopy for Geochemical Characterization of Shale Reservoirs

The hydrocarbon-generating potential of source rocks can be assessed by tracking physical and chemical changes in the molecular structure of kerogen through thermal maturation. Since, compared with other carbonaceous materials, the complex kerogen structure is closely related to its maturity (Khatibi et al. 2018).

By increasing maturity structural changes take place in organic matter which can be detected by Raman Spectroscopy and yield valuable information. When kerogen undergoes maturity, its aromaticity will increase which is followed by a shift in the position of the D band (as disorder band) towards lower wavelength and lower

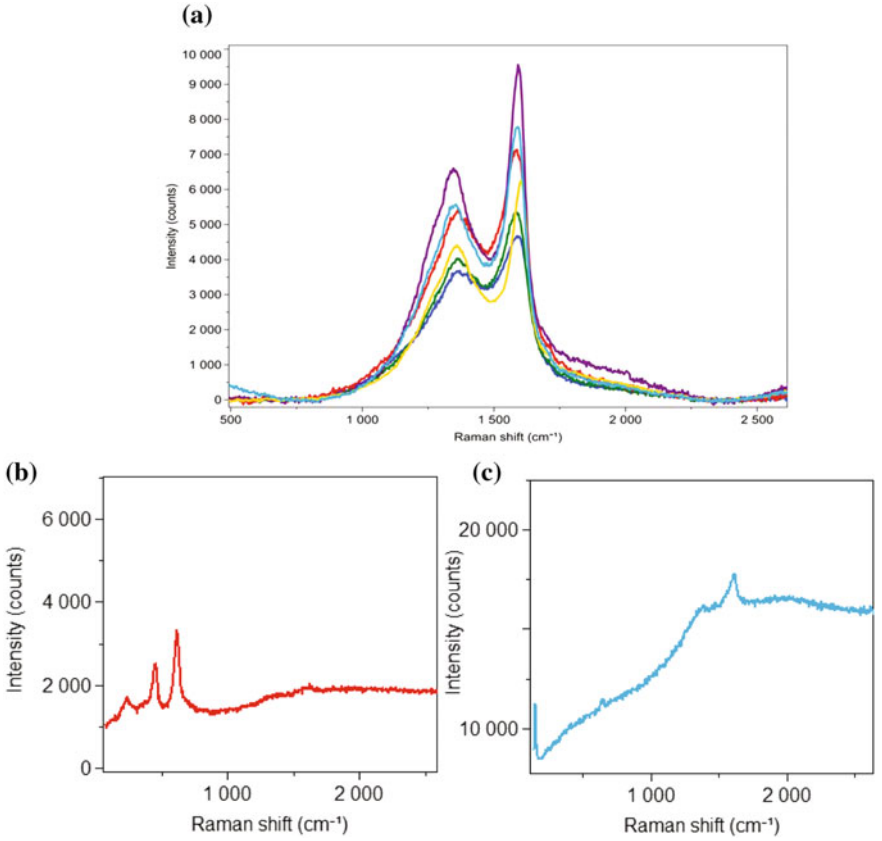

Fig. 3.4 **a** Raman spectra of six different samples with different maturity levels. Note the two major bands and also change of band position and amplitude for each sample, **b**, **c** other peaks corresponding to other components in organic rich shale

intensities. This shift is attributed to the increase of larger aromatic clusters and more ordered-structure kerogen (Schito et al. 2017; Khatibi et al. 2018). While, changes for G band position is a slight shift towards higher wavelength. This process allows for Raman to detect different levels of maturation by considering band separation (the distance between two major bands), Fig. 3.5. At initial stages of maturation, band separation increases with a higher intensity while this rapid growth tapers off over higher maturities. This might be explained by the fact that cracking of organic matter before the peak oil window is faster than the post peak oil window (Khatibi et al. 2018). Gao et al. (2017) detected abrupt changes in the structure of kerogen before the peak oil window and at the end of the oil window by the artificial maturation of oil shale kerogen. The sudden drop in HI during the peak oil window also supports the elimination of the oil potential from the kerogen residue. Consequently, after the oil window, structural changes decrease which can be reflected by the slope of line in Fig. 3.5.

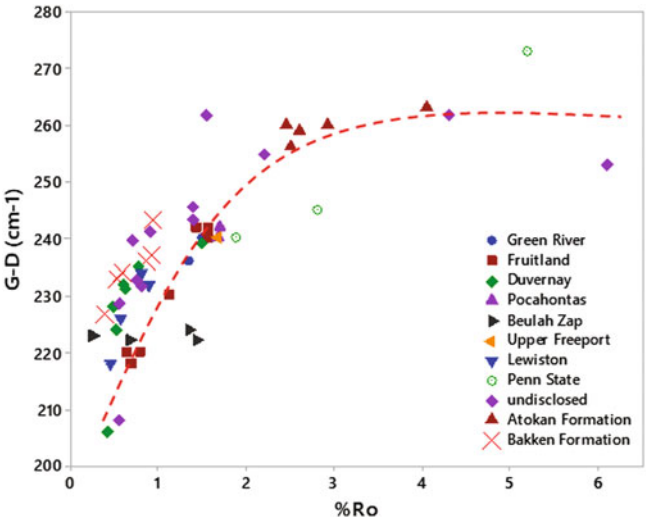

Fig. 3.5 Band separation of major Raman spectroscopy bands versus maturity for 12 different fields

Table 3.2 Average values of TOC content, vitrinite reflectance, hydrogen index, IR aliphatic carbon content, and NMR carbon aromaticity. As seen, by increasing maturity, HI and aliphatic carbon decrease, while aromaticity increases. *Source* modified from Witte et al. (1988)

TOC (wt%)	% VRo	HI (mg HC/gr rock * gr TOC)	Aliphatic carbon (mg aliph. C/gr rock)	Carbon aromaticity (from NMR)
10.56	0.48	664	47.8	0.33
7.83	0.66	642	38.5	0.43
6.16	0.88	361	22.5	0.60
5.90	1.45	74	10.1	0.80

Major molecules in kerogen are aromatics linked by aliphatic and heteroatomic moieties (Kelemen and Fang 2001) in which solid bitumen (soluble in organic solvents) may be trapped as well (Wopenka and Pasteris 1993). During hydrocarbon generation, many of the aliphatic carbon linkages are lost. The aliphatic portion of organic matter is the main contributor for hydrocarbon production (Witte et al. 1988; Schenk et al. 1986; Gao et al. 2017) which can be attributed to S2 peak in the Rock-Eval analysis which represents the potential of kerogen to produce hydrocarbons. These structural changes can be detected by different spectroscopy methods (Quirico et al. 2005). Witte et al. (1988) used Infrared Spectroscopy (IR) to show that aliphatic carbon concentrations decrease with an increase in maturity of the samples, Table 3.2. Gao et al. (2017) exposed the samples to artificial maturation and presented that mostly, CH_2 groups (aliphatic) are the contributing compound to the hydrocarbon generation using quantitative ^{13}C DP MAS NMR spectra.

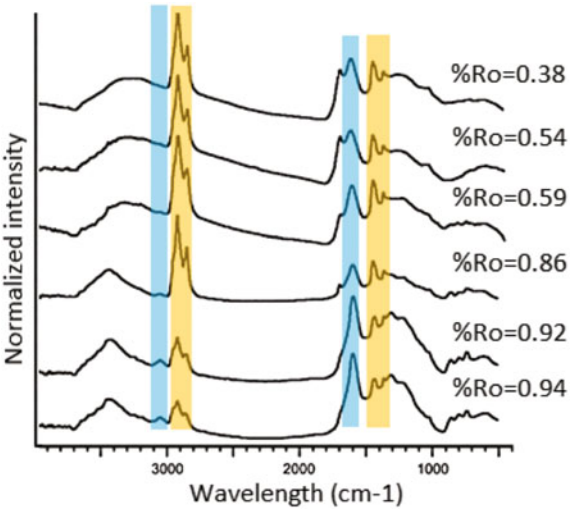

Fig. 3.6 FTIR spectra of kerogens with increasing maturity exhibit increasing aromatic absorption (blue area) and decreasing aliphatic absorption (orange area)

Fourier Transform InfraRed (FTIR), the preferred method of infrared spectroscopy, can be used to identify chemical compounds in organic materials and verify the results from the Raman spectroscopy. Figure 3.6 shows how FTIR spectra of kerogens with increasing maturity exhibit increasing aromatic absorption, decreasing aliphatic absorption for six samples with natural maturity level. Chen et al. (2015) also used micro-FTIR chemistry map of integrated peak area of aliphatic CH_x groups on Shale samples at different maturity levels (by artificial maturation procedure). They showed, in response to the increase in thermal stress, convertible carbon gradually transforms into hydrocarbons that can later be expelled from the rock, and consequently, the intensity of aliphatic groups decreases, as evidenced by the low intensity of aliphatic IR absorbance in highly mature samples.

This notable change in kerogen molecular structure and clustering of aromatics were also detected by Quirico et al. (2005) using high-resolution transmission electronic microscope (TEM). By increasing maturity, the number of stacked aromatic layers slightly increases, and onion ring microtexture will be visible for higher mature samples (Beyssac et al. 2002).

Such structural change can also be detected by Raman spectroscopy (Wang et al. 1990) and related to other properties. As mentioned before, the origin of the G band in Raman spectroscopy is because of the inplane E_{2g2} vibrational modes of the carbon atoms in aromatic ring structures (Beyssac et al. 2002, 2003; Sauerer et al 2017). The abundance of aromatic structures means less potential to produce hydrocarbon, thus, S2 from Rock-Eval can be correlated to G band from Raman spectroscopy, Fig. 3.7.

During the maturation and increase in produced hydrocarbons, the heteroatom-rich organic precursors lose many of their oxygenated and hydrogenated chemical groups (Oberlin et al. 1980; Rouzaud and Oberlin 1989) and attachments separating

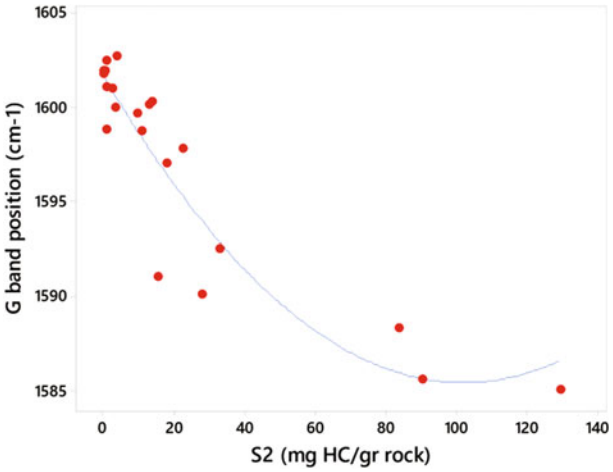

Fig. 3.7 G band position versus S2 from Rock-Eval

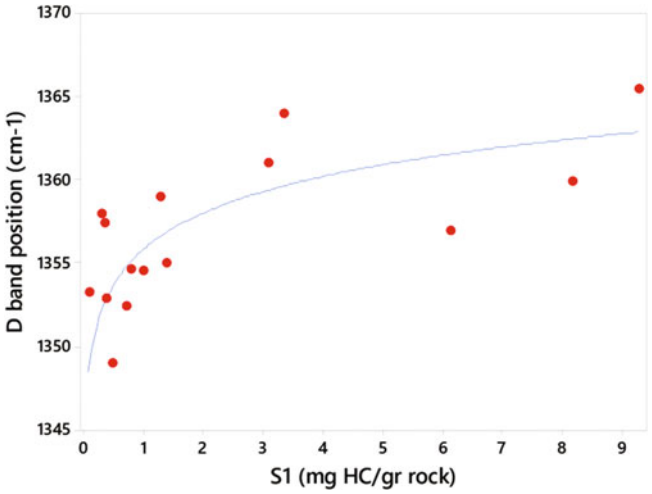

Fig. 3.8 D band position versus S1 from Rock-Eval

from aromatic carbons increases (Kelemen and Fang 2001). It was mentioned earlier that D band refers to a disorder in the atoms which is resultant from the Raman-active A_{1g} symmetry associated with in-plane lattice defects and discontinuities of the sp^2 carbon network like heteroatoms (Sauerer et al. 2017). Therefore, D band from Raman spectroscopy can be used as a measure of attachments separated from organic matter which is concurrent with hydrocarbon generation. This process can be presented by S1 peak in Rock-Eval, Fig. 3.8.

In addition to geochemical properties of organic matter, Raman spectroscopy has the potential to predict the mechanical property of organic matter in terms of Young's modulus (Khatibi et al. 2018). This method is helpful since kerogen is dispersed in the rock matrix and conventional mechanical properties measurements in literature on core samples (Aghajanpour et al. 2017) cannot be performed on organic matter.

It is believed that in immature source rock samples, the organic matter appears to surround other minerals, becoming a load-bearing part of the rock framework. However, as the maturity increases, kerogen becomes more isolated among other grains (Zargari et al. 2011; Dietrich 2015; Khatibi et al. 2018) and its Young's modulus increases. Few studies have been able to confirm this interpretation by direct measurement (Emmanuel et al. 2016; Li et al. 2017), Fig. 3.9. This phenomenon can be discussed from a molecular point of view. When maturity happens, kerogen loses heteroatoms (O, S and N) and its aliphatic carbons (hydrogen-rich groups). The residue is a hydrogen-poor structure molecule, which is dominated by aromatic carbons. During the process of maturation, which increases with burial depth, pore-walls rupture. This sequence promotes the mechanical reorientation and alignment of the aromatic units, thus will facilitate the reduction of defects (Khatibi et al. 2018). This is due to diffusion, elimination of bonding vacancies and annealing of aromatic sheets to triperiodic graphite (Bustin 1996). Therefore, from the early stages of maturation, the macromolecule arrangements transform gradually from the chaotic and mixed layers to a more ordered arrangement (Pan et al. 2013; Khatibi et al. 2018).

Considering the relationship that exists between Raman spectra versus maturity, Fig. 3.5, and Young's modulus versus maturity, Fig. 3.9, Raman data can be used

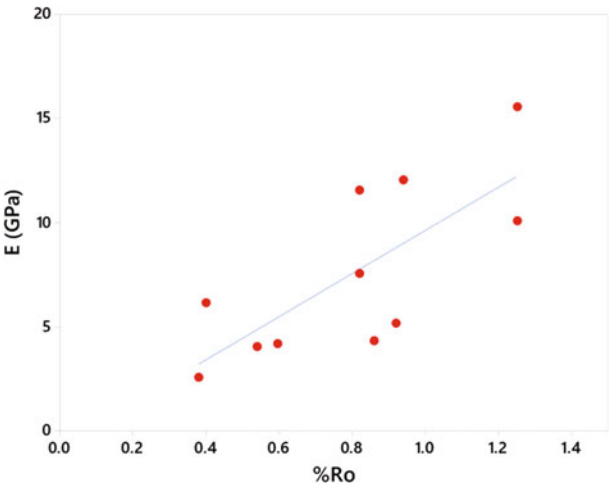

Fig. 3.9 Maturity versus Young's modulus for two different datasets. Note the general increasing trend in Young's modulus by increasing maturity

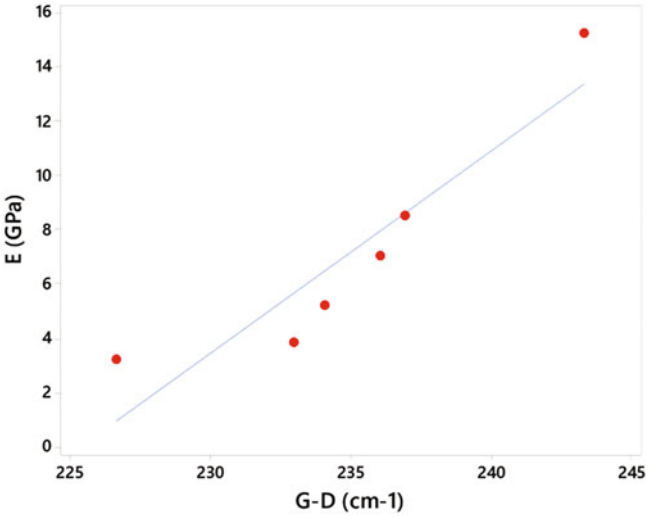

Fig. 3.10 Young's modulus versus band separation. Considering the relationship that exists between maturity and Raman spectra, and maturity with Young's modulus, Raman data can be used as an indirect method to study the mechanical properties of organic matter

as an indirect method to study the mechanical properties of organic matter (Khatibi et al. 2018), Fig. 3.10.

It was shown in Fig. 3.5 when %Ro varies from 0.3 to 3 (initial stages of maturation to the late dry gas window), band separation varies approximately between 210 and 255 cm^{-1}, respectively. Based on correlation in Fig. 3.10, Young's modulus (E) can be estimated approximately from 0.32 to 40 GPa for organic matter (Khatibi et al. 2018). This is in line with previous results by Eliyahu et al. (2015) who predicted Young's modulus of organic matter in the range of 0–25 GPa for maturities up to %Ro = 2.1.

What mentioned above was a brief introduction to different methods for characterizing organic matter and discussing employing new methods such as Raman spectroscopy in the study of shale reservoirs. High resolution for the laser focal volume of the Raman equipment (around 3 μm^3) allows for the analysis of small volumes of dispersed organic material with good precision. Furthermore, the minimal and rapid sample preparation for Raman spectroscopy enables acquiring Raman spectrum in minutes.

References

Aghajanpour A, Fallahzadeh SH, Khatibi S, Hossain MM, Kadkhodaie A (2017) Full waveform acoustic data as an aid in reducing uncertainty of mud window design in the absence of leak-off test. J Nat Gas Sci Eng 45:786–796

Amer M (2009) Raman spectroscopy for soft matter applications. Wiley, USA
Behar F, Beaumont V, Penteado HDB (2001) Rock-Eval 6 technology: performances and developments. Oil Gas Sci Technol 56:111–134
Beyssac O, Goffé B, Chopin C, Rouzaud J (2002) Raman spectra of carbonaceous material in metasediments: a new geothermometer. J Metamorph Geol 20:859–871
Beyssac O, Goffé B, Petitet J-P, Froigneux E, Moreau M, Rouzaud JN (2003) On the characterization of disordered and heterogeneous carbonaceous materials by Raman spectroscopy. Spectrochim Acta A 59(10):2267–2276
Bustin R (1996) Mechanisms of graphite formation from kerogen: experimental evidence. In: Fuel and energy abstracts. Elsevier, p 187
Carvajal-Ortiz H, Gentzis T (2015) Critical considerations when assessing hydrocarbon plays using Rock-Eval pyrolysis and organic petrology data: data quality revisited. Int J Coal Geol 152:113–122
Cesare B, Maineri C (1999) Fluid-present anatexis of metapelites at El Joyazo (SE Spain): constraints from Raman spectroscopy of graphite. Contrib Minerl Petrol 135:41–52
Chen Y, Zou C, Mastalerz M, Suyun H, Gasaway C, Tao X (2015) Applications of micro-fourier transform infrared spectroscopy (FTIR) in the geological sciences—a review. Int J Mol Sci 16 (12):30223–30250
Diessel C, Brothers R, Black P (1978) Coalification and graphitization in high-pressure schists in New Caledonia. Contrib Minerl Petrol 68:63–78
Dietrich AB (2015) The impact of organic matter on geomechanical properties and elastic anisotropy in the Vaca Muerta shale. PhD dissertation, Colorado School of Mines, Arthur Lakes Library
Eliyahu M, Emmanuel S, Day-Stirrat RJ, Macaulay CI (2015) Mechanical properties of organic matter in shales mapped at the nanometer scale. Mar Pet Geol 59:294–304
Emmanuel S, Eliyahu M, Day-Stirrat RJ, Hofmann R, Macaulay CI (2016) Impact of thermal maturation on nano-scale elastic properties of organic matter in shales. Mar Pet Geol 70:175–184
Espitalie J, Deroo G, Marquis F (1985) Rock-Eval pyrolysis and its applications. Rev De L Institut Fr Du Pet 40:563–579
Gao Y, Zou Y-R, Liang T, Peng PA (2017) Jump in the structure of type I kerogen revealed from pyrolysis and 13C DP MAS NMR. Org Geochem 112:105–118
Hackley PC, Araujo CV, Borrego AG, Bouzinos A, Cardott BJ, Cook AC, Eble C, Flores D, Gentzis T, Gonçalves PA (2015) Standardization of reflectance measurements in dispersed organic matter: results of an exercise to improve interlaboratory agreement. Mar Pet Geol 59:22–34
Huang E-P, Huang E, Yu S-C, Chen Y-H, Lee J-S, Fang J-N (2010) In situ Raman spectroscopy on kerogen at high temperatures and high pressures. Phys Chem Miner 37:593–600
Hutton A, Bharati S, Robl T (1994) Chemical and petrographic classification of kerogen/macerals. Energy Fuels 8:1478–1488
Jacob H (1989) Classification, structure, genesis and practical importance of natural solid oil bitumen ("migrabitumen"). Int J Coal Geol 11:65–79
Jarvie D, Claxton B, Henk B, Breyer J (2001) Oil and shale gas from Barnett shale, Ft. In: Worth basin, TX, poster presented at the AAPG national convention, Denver, CO
Kelemen S, Fang H (2001) Maturity trends in Raman spectra from kerogen and coal. Energy Fuels 15:653–658
Khatibi S, Ostadhassan M, Tuschel D, Gentzis T, Bubach B, Carvajal-Ortiz H (2018) Raman spectroscopy to study thermal maturity and elastic modulus of kerogen. Int J Coal Geol 185:103–118
Lafargue E, Marquis F, Pillot D (1998) Rock-Eval 6 applications in hydrocarbon exploration, production, and soil contamination studies. Rev De L'Institut Fr Du Pét 53:421–437
Li C, Ostadhassan M, Kong L (2017) Nanochemo-mechanical characterization of organic shale through AFM and EDS. In: 2017 SEG international exposition and annual meeting. Society of Exploration Geophysicists

Marshall CP, Edwards HG, Jehlicka J (2010) Understanding the application of Raman spectroscopy to the detection of traces of life. Astrobiology 10:229–243

Mitra SS (1962) Vibration spectra of solids. In: Solid state physics, vol 13. Academic Press, pp 1–80

Oberlin A, Boulmier J, Villey M (1980) Electron microscopic study of kerogen microtexture. Selected criteria for determining the evolution path and evolution stage of kerogen. In: Kerogen: Insoluble organic matter from sedimentary rocks. Editions Technip, Paris, pp 191–241

Pan J, Meng Z, Hou Q, Ju Y, Cao Y (2013) Coal strength and Young's modulus related to coal rank, compressional velocity and maceral composition. J Struct Geol 54:129–135

Peters K (1986) Guidelines for evaluating petroleum source rock using programmed pyrolysis. AAPG Bull 70:318–329

Quirico E, Rouzaud J-N, Bonal L, Montagnac G (2005) Maturation grade of coals as revealed by Raman spectroscopy: progress and problems. Spectrochim Acta Part A Mol Biomol Spectrosc 61:2368–2377

Reich S, Thomsen C (2004) Raman spectroscopy of graphite. Philos Trans R Soc Lond A Math Phys Eng Sci 362:2271–2288

Rouzaud J, Oberlin A (1989) Structure, microtexture, and optical properties of anthracene and saccharose-based carbons. Carbon 27:517–529

Sauerer B, Craddock PR, AlJohani MD, Alsamadony KL, Abdallah W (2017) Fast and accurate shale maturity determination by Raman spectroscopy measurement with minimal sample preparation. Int J Coal Geol 173:150–157

Schenk H, Witte E, Müller P, Schwochau K (1986) Infrared estimates of aliphatic kerogen carbon in sedimentary rocks. Org Geochem 10:1099–1104

Schito A, Romano C, Corrado S, Grigo D, Poe B (2017) Diagenetic thermal evolution of organic matter by Raman spectroscopy. Org Geochem 106:57–67

Tuschel D (2013) Raman spectroscopy of oil shale. Spectroscopy 28:5

Wang Y, Alsmeyer DC, McCreery RL (1990) Raman spectroscopy of carbon materials: structural basis of observed spectra. Chem Mater 2:557–563

Witte E, Schenk H, Müller P, Schwochau K (1988) Structural modifications of kerogen during natural evolution as derived from 13C CP/MAS NMR, IR spectroscopy and Rock-Eval pyrolysis of Toarcian shales. Org Geochem 13:1039–1044

Wopenka B, Pasteris JD (1993) Structural characterization of kerogens to granulite-facies graphite: applicability of Raman microprobe spectroscopy. Am Mineral 78:533–557

Zargari S, Prasad M, Mba KC, Mattson E (2011) Organic maturity, hydrous pyrolysis, and elastic property in shales. In: Canadian unconventional resources conference. Society of Petroleum Engineers